

# RESEARCH MEMORANDUM

WIND-TUNNEL INVESTIGATION OF THE DAMPING IN ROLL  
OF THE BELL X-1E RESEARCH AIRPLANE AND ITS  
COMPONENTS AT SUPERSONIC SPEEDS

By Russell W. McDearmon and Frank L. Clark

Langley Aeronautical Laboratory  
Langley Field, Va.

NATIONAL ADVISORY COMMITTEE  
FOR AERONAUTICS  
WASHINGTON

April 26, 1956  
Declassified October 28, 1960

NATIONAL ADVISORY COMMITTEE FOR AERONAUTICS

RESEARCH MEMORANDUM

WIND-TUNNEL INVESTIGATION OF THE DAMPING IN ROLL  
OF THE BELL X-1E RESEARCH AIRPLANE AND ITS  
COMPONENTS AT SUPERSONIC SPEEDS

By Russell W. McDearmon and Frank L. Clark

SUMMARY

Experimental values of the damping in roll at zero angle of attack of the Bell X-1E research airplane and various combinations of its components have been obtained at Mach numbers of 1.62, 1.94, 2.22, 2.41, and 2.62.

The damping in roll of the complete model was of the order predicted by theory. Very slight and gradual decreases in the damping in roll were obtained as the Mach number was increased from 1.62 to 2.41, followed by a somewhat more abrupt decrease as the Mach number was increased from 2.41 to 2.62. The wing was the predominant contributor to the damping in roll throughout the Mach number range of the tests. The dorsal and ventral fins had little effect on the damping in roll of the complete model.

INTRODUCTION

The only wind-tunnel data available on the aerodynamic characteristics of the Bell X-1E research airplane have been in the subsonic and transonic speed ranges. In order to supply information at supersonic speeds, a general program of investigations is being undertaken in the Langley 9-inch supersonic tunnel to determine some of the dynamic and static stability characteristics of the X-1E.

In the present investigation, the damping in roll at zero angle of attack of the complete airplane and various combinations of its components was obtained at Mach numbers of 1.62, 1.94, 2.22, 2.41, and 2.62. Included were determinations of the effects of the dorsal and ventral fins on the damping in roll. In this report, the term "dorsal fin" includes the

canopy and the conduit which extends rearward from the canopy and is faired smoothly into the vertical tail. The term "ventral fin" refers to the smaller conduit which extends along a major portion of the underside of the body. Comparisons were made with some theoretical predictions.

## SYMBOLS

b	wing span, ft
$C_l$	rolling-moment coefficient, $M_x/qSb$
$C_{l_p}$	damping-in-roll derivative, $\frac{\partial C_l}{\partial \frac{pb}{2V}}$
$M_x$	rolling moment, ft-lb
M	free-stream Mach number
p	rolling angular velocity, radians/sec
$pb/2V$	wing-tip helix angle, radians
q	free-stream dynamic pressure, lb/sq ft
S	total wing area, including portion submerged in body, sq ft
V	free-stream velocity, ft/sec

## Configuration identification:

BW	body and wing
BV	body and vertical tail
BVH	body, vertical tail, and horizontal tail
BWV	body, wing, and vertical tail
BWVH	body, wing, vertical tail, and horizontal tail

## APPARATUS

## Wind Tunnel

All investigations were conducted in the Langley 9-inch supersonic tunnel which is a closed-circuit, continuous-operation type in which stream pressure, temperature, and humidity can be controlled at all times during tunnel operation. Different test Mach numbers are provided by interchangeable nozzle blocks which form test sections approximately 9 inches square. Eleven fine-mesh turbulence-damping screens are installed in the settling chamber ahead of the supersonic nozzle. The turbulence level of the tunnel is considered low, based on past turbulence-level measurements.

## Models, Support, and Rolling-Moment Balance

A drawing of the complete 1/62-scale model of the X-1E is presented in figure 1. The sting was an integral part of the model body. In order to use a sting of sufficient strength to withstand the forces which would be encountered in testing, it was necessary to alter the shape of the rear portion of the body, as shown in figure 1. The effect of this alteration on  $C_{L_p}$  was believed to be negligible.

In order to attain high rotational speeds with a minimum of model vibration in testing, it was necessary that the models be carefully mass-balanced and be lightweight, commensurate with strength requirements. Three identical bodies were constructed, one for the BWVH and BWV configurations, one for the BW configuration, and one for the BV and BVH configurations. Three bodies were required so that BWVH, BW, and BVH could be mass-balanced separately by inserting lead weights at various positions along each body. Configurations BWV and BV were not mass-balanced separately, since the effect of the horizontal tail on the mass-balancing was negligible. One wing, one vertical tail, and one vertical-tail—horizontal-tail unit were made. Each of these was removable, so that it could be installed on the desired body. The nose portions of the bodies were made of aluminum. The remaining portions of the bodies, the integral stings, and the wings were made of steel. The tail panels and the dorsal and ventral fins were molded from plastic materials. When the dorsal and ventral fins were removed, the body became a body of revolution, and the vertical tail was faired smoothly into the body, as shown in figure 1.

Transition strips of aluminum oxide particles were placed on the components of all models. These strips were approximately 0.006 inch thick and were located as shown in figure 1.

Since the tail panels were molded from plastic materials, they may have experienced slight bending or twisting when tested. However, the resulting aeroelastic effect on the contributions of the tail panels to  $C_{L_p}$  is believed to have been small.

Photographs of the damping-in-roll test apparatus are presented in figure 2. (The model shown in fig. 2(a) is the Bell X-1A model used in the investigation of ref. 1. In all other respects the tunnel setup used in ref. 1 and that used in the present investigation are identical.) The model sting was inserted into the spindle of the rolling-moment balance and secured by a Woodruff key and setscrews. The spindle was rotated by means of gears and an electric motor outside the tunnel. The rolling velocity was measured with a Strobocorr frequency indicator which was modified to indicate revolutions per minute by means of a generator attached to the rear of the spindle. The rolling moments were measured by strain gages on the spindle and were transmitted through slip rings and brushes to a Brown self-balancing potentiometer outside the tunnel.

#### TESTS

The damping in roll at zero angle of attack was obtained at Mach numbers of 1.62, 1.94, 2.22, 2.41, and 2.62 for the configurations listed in the following table:

Configuration	Dorsal fin	Ventral fin
BWVH	On	On
BWVH	Off	Off
BWVH	On	Off
BWV	On	On
BW	On	On
BW	Off	Off
BV	On	On
BVH	On	On

The test Reynolds number range for the BWVH configurations was from  $0.33 \times 10^6$  to  $0.62 \times 10^6$ , based on the mean aerodynamic chord of the wing. However, all tests were conducted with transition strips on the components to create a turbulent boundary layer over most of the model and thereby more closely simulate full-scale conditions. The effectiveness of similar transition strips in creating a turbulent boundary layer may be seen in reference 2.

## PRECISION

The precision of the data has been determined by estimating the accuracies of the measured quantities and evaluating their effects on the coefficient  $C_L$  and the parameter  $pb/2V$ . The probable error in the strain-gage indication produced the following errors in  $C_L$ :

M	Error in $C_L$ for configuration -	
	BWVH, BWV, BW	BVH, BV
1.62	$\pm 0.00030$	$\pm 0.00015$
1.94	$\pm 0.00034$	$\pm 0.00018$
2.22	$\pm 0.00041$	$\pm 0.00020$
2.41	$\pm 0.00026$	$\pm 0.00022$
2.62	$\pm 0.00028$	$\pm 0.00025$

Error in the measurement of the rolling velocity caused a maximum error in  $pb/2V$  of  $\pm 0.00009$ . The surveyed variation of each of the free-stream Mach numbers was approximately  $\pm 0.01$ , which produced a maximum error in  $pb/2V$  of  $\pm 0.00010$ . Thus the maximum total error in  $pb/2V$  was  $\pm 0.00019$ .

Model alignment was maintained to within  $\pm 0.1^\circ$  of zero pitch and yaw with respect to the tunnel center line.

The rolling-moment balance was statically calibrated, before and at intervals during the testing, to ascertain that there were no changes in the strain-gage constant. Throughout the tests, the moisture content in the tunnel was kept sufficiently low to insure that the effects of condensation were negligible.

## RESULTS AND DISCUSSION

The variations of rolling-moment coefficient with wing-tip helix angle for the various configurations are presented in figure 3. In general, the variations were linear.

The Contributions of the Airplane Components to  $C_{Lp}$ 

The variations with Mach number of  $C_{Lp}$  for the complete model and its components are presented in figure 4. The values of  $C_{Lp}$  were

obtained by taking the slopes of the variations of  $C_l$  with  $pb/2V$  presented in figure 3.

For the complete model, a very slight and gradual decrease in the damping in roll was obtained as the Mach number was increased from 1.62 to 2.41, followed by a somewhat more abrupt decrease as the Mach number was increased from 2.41 to 2.62. The dorsal and ventral fins had little effect on the damping of the complete model.

The wing was the predominant contributor to  $C_{lp}$  throughout the Mach number range of the tests, although the contributions of the tail panels to  $C_{lp}$  and interference effects of the dorsal and ventral fins were in some instances significant, especially near  $M = 1.94$ . It is interesting to note that at  $M = 1.62$  and  $1.94$  the contribution of the horizontal tail was markedly affected by the wing; the addition of the horizontal tail to BWV increased the damping, but the addition of the horizontal tail to BV decreased the damping. At Mach numbers greater than  $1.94$ , the addition of the horizontal tail to BV had very little effect on  $C_{lp}$ .

#### Comparisons of the Experimental Values of $C_{lp}$ With

#### Some Theoretical Predictions

The experimental variations of  $C_{lp}$  with  $M$  are compared with some theoretical variations for the complete model and its components in figure 5. The theoretical predictions were obtained by the method employed in reference 1. This method consisted of predictions by linear theory of  $C_{lp}$  for the wing and tail panels (shown individually in figs. 5(b) and 5(c)) plus approximations of the effects of the wing flow field on the tail panels. The effect of the interference field from the body on  $C_{lp}$  was neglected.

The general levels of  $C_{lp}$  obtained experimentally for all the configurations were of the order predicted by theory. However, in the Mach number region from 2.22 to 2.41 the experimental damping in roll was greater than that predicted theoretically for all configurations containing the wing. This contrasts with the results obtained in reference 1 for the Bell X-1A research airplane. In reference 1, the experimental damping of the BWVH and BWV configurations was considerably less than that predicted by theory in the Mach number range from 2.22 to 2.41.

Although theory underestimated the damping at Mach numbers of 2.22 and 2.41 for all configurations containing the wing, at a Mach number of 1.62, theory overestimated the damping. Also, from the trend established by the test results, it appears that at Mach numbers greater than 2.62, theory will again overestimate the damping.

#### CONCLUDING REMARKS

Wind-tunnel investigations of the damping in roll at zero angle of attack of the Bell X-1E research airplane and various combinations of its components were made at Mach numbers of 1.62, 1.94, 2.22, 2.41, and 2.62.

The damping in roll of the complete model was of the order predicted by theory. Very slight and gradual decreases in the damping in roll were obtained as the Mach number was increased from 1.62 to 2.41, followed by a somewhat more abrupt decrease as the Mach number was increased from 2.41 to 2.62. The wing was the predominant contributor to the damping in roll throughout the Mach number range of the tests. The dorsal and ventral fins had little effect on the damping in roll of the complete model.

Langley Aeronautical Laboratory,  
National Advisory Committee for Aeronautics,  
Langley Field, Va., February 2, 1956.



## REFERENCES

1. McDearmon, Russell W., and Clark, Frank L.: Wind-Tunnel Investigation of the Damping in Roll of the Bell X-1A Research Airplane and Its Components at Supersonic Speeds. NACA RM L55I19, 1956.
2. Fallis, William B.: On Distributed Roughness as a Means of Fixing Transition at High Supersonic Speeds. Jour. Aero. Sci. (Readers' Forum), vol. 22, no. 5, May 1955, p. 339.

7-8d108

Wing:

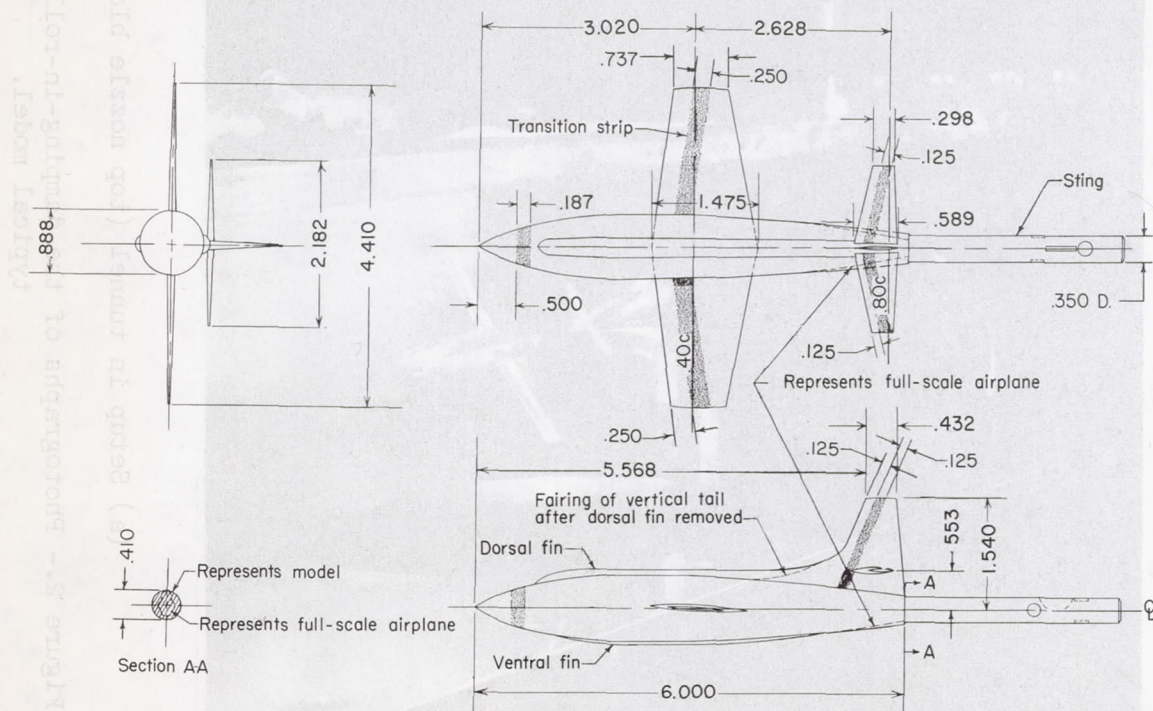
Area	4.864 sq. in.
Span	4.410 in.
Aspect ratio	4
Section	modified 64A004
Root incidence	2°
Tip incidence	2°

Horizontal tail:

Area	0.974 sq. in.
Section	65-008

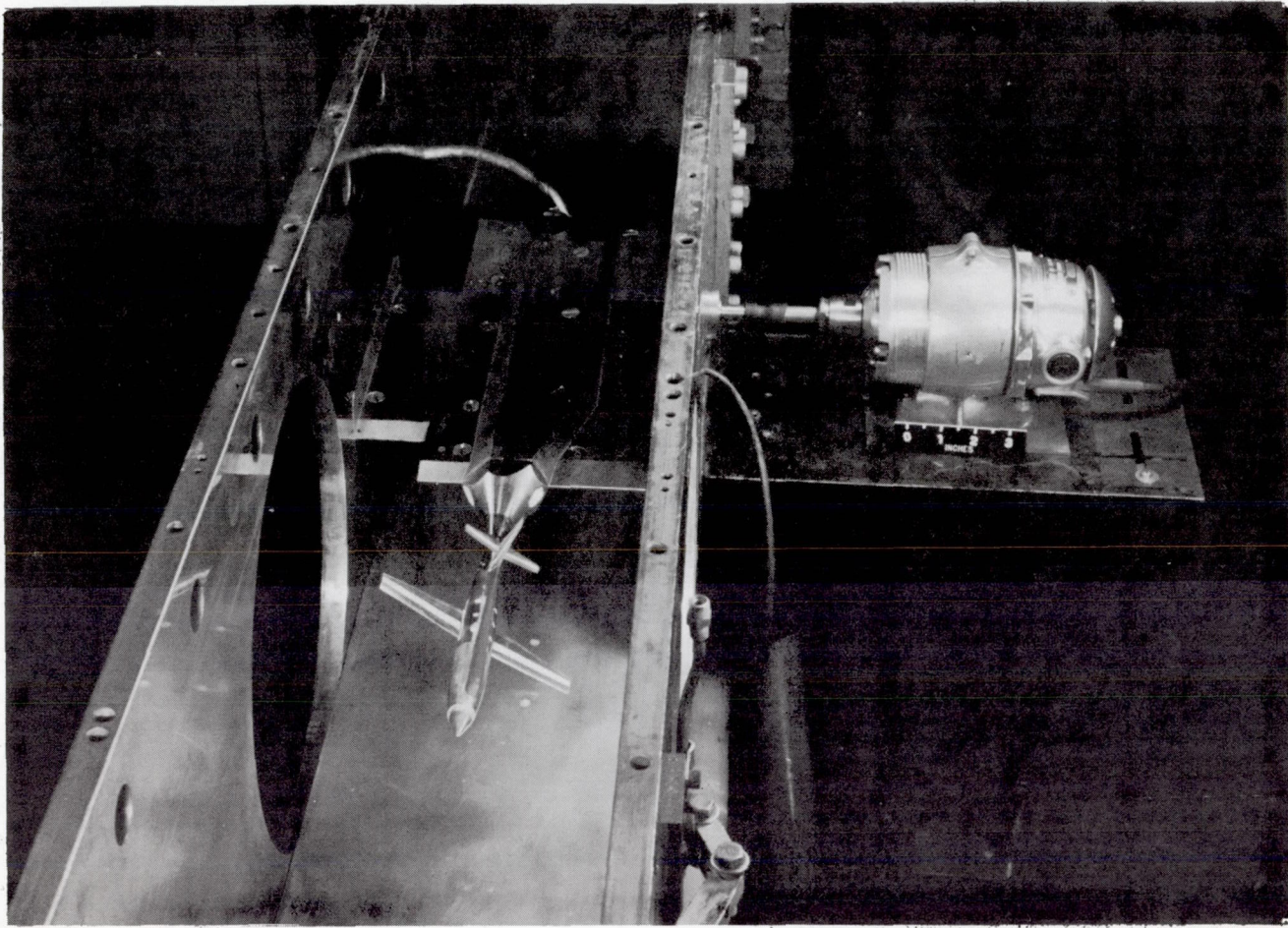
Vertical tail:

Area	0.958 sq. in.
Section	65-008



Note: all dimensions are in inches.

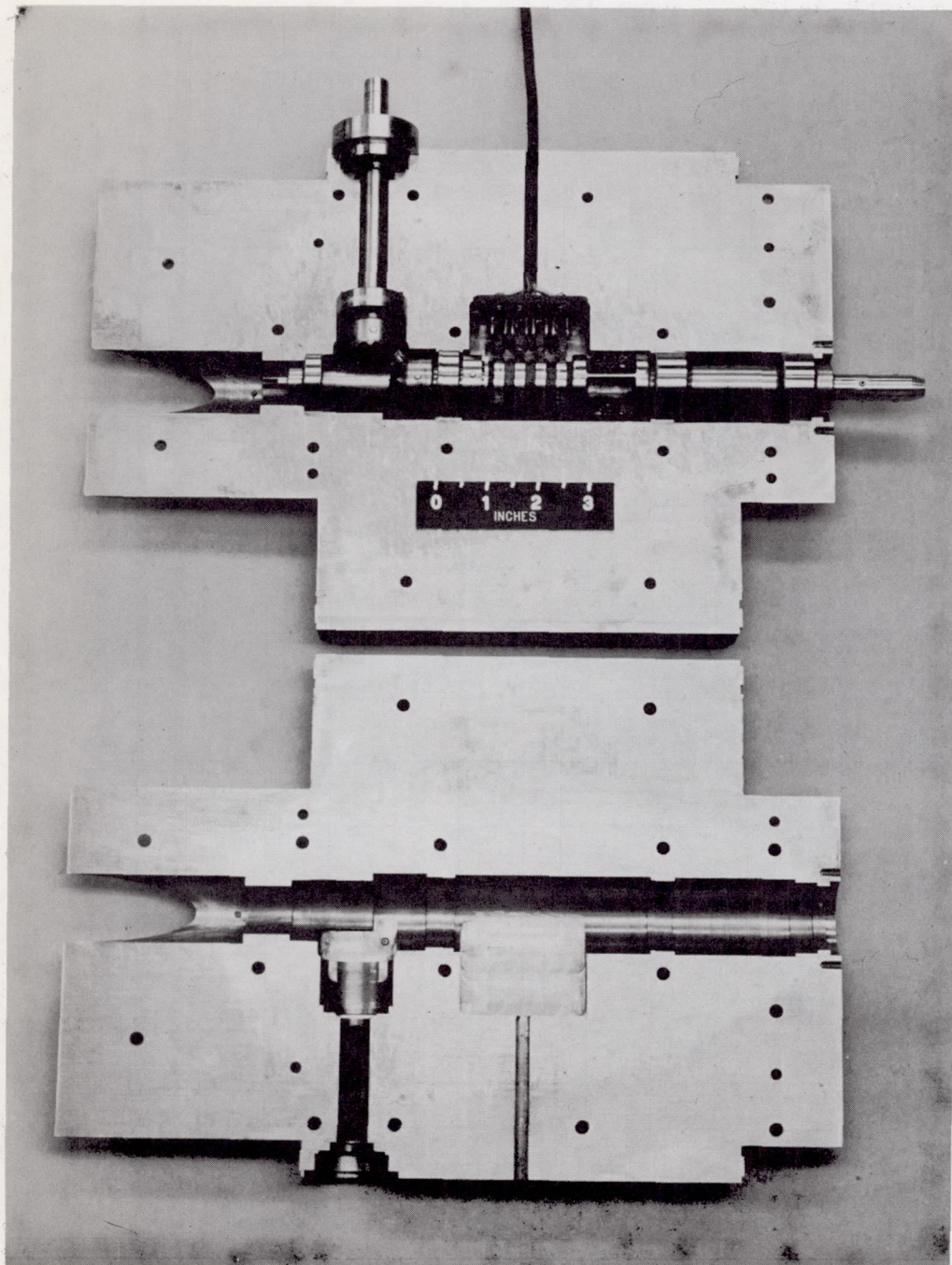
Figure 1.- Drawing of the complete model.



(a) Setup in tunnel (top nozzle block removed).

L-89408

Figure 2.- Photographs of the damping-in-roll test apparatus and a typical model.



(b) Interior of balance.

L-89409

Figure 2.- Concluded.

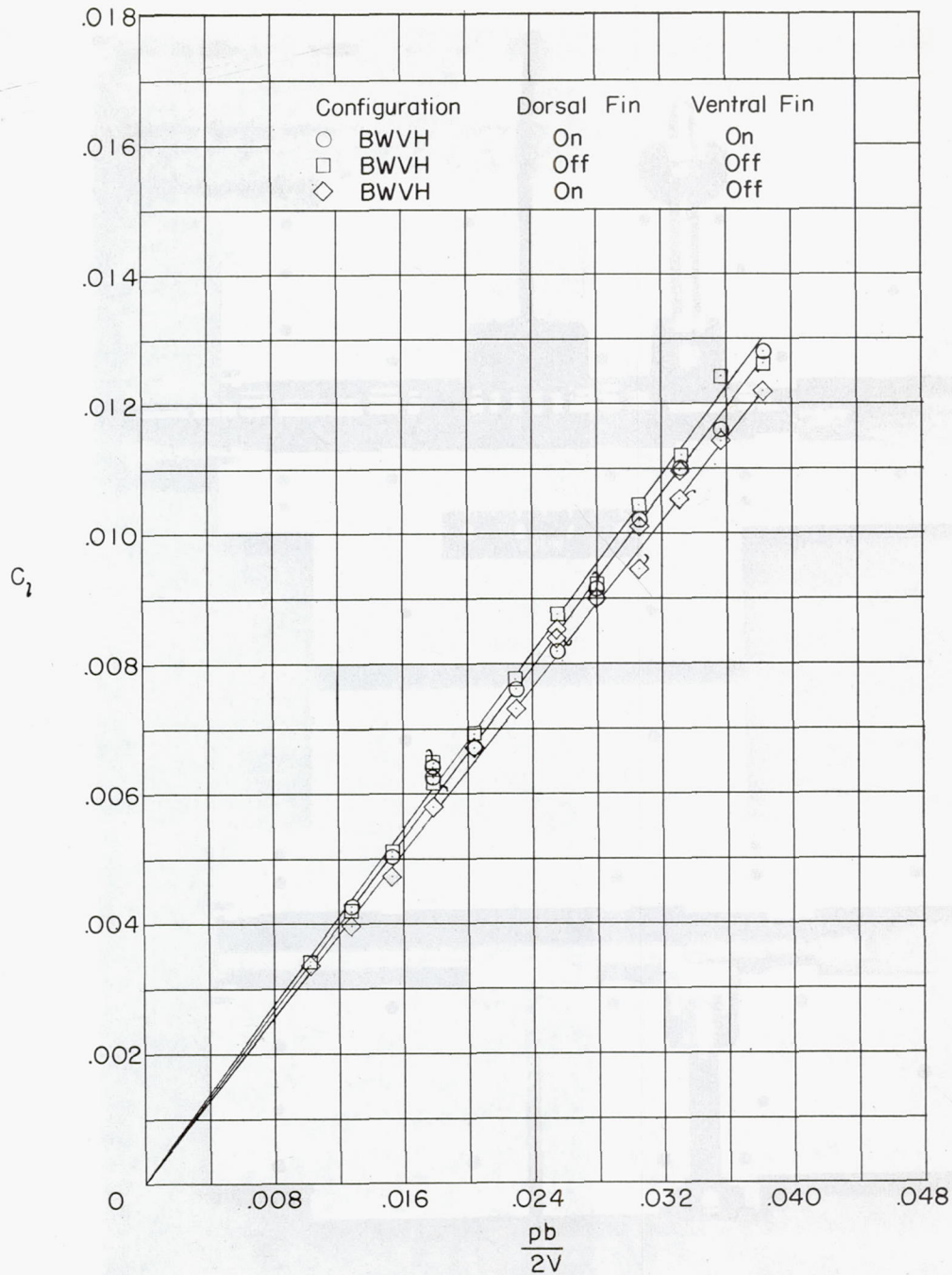
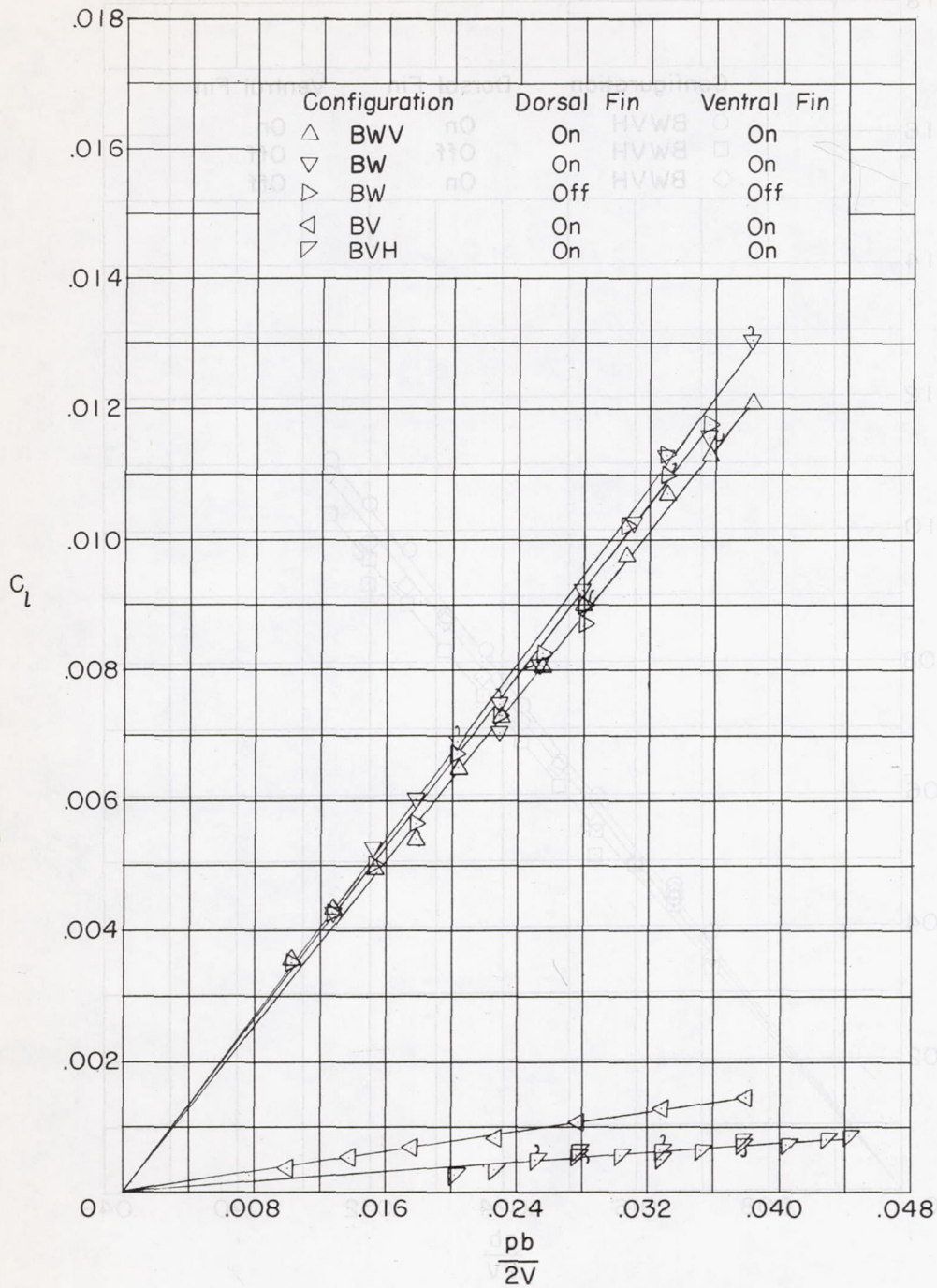
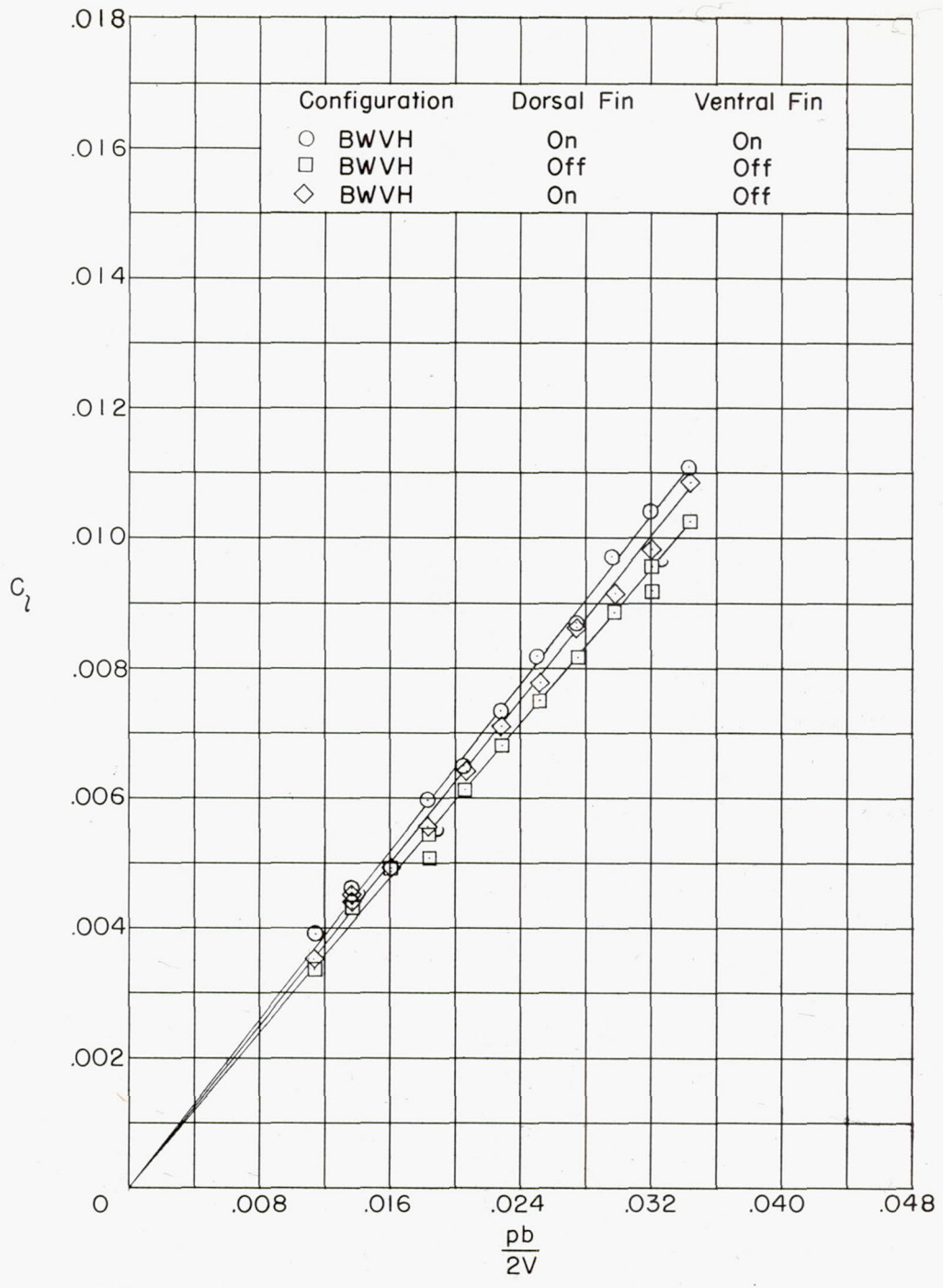
(a)  $M = 1.62$ .

Figure 3.- Variations of rolling-moment coefficient with wing-tip helix angle of the complete model and its components at zero angle of attack. Flagged symbols indicate check points.



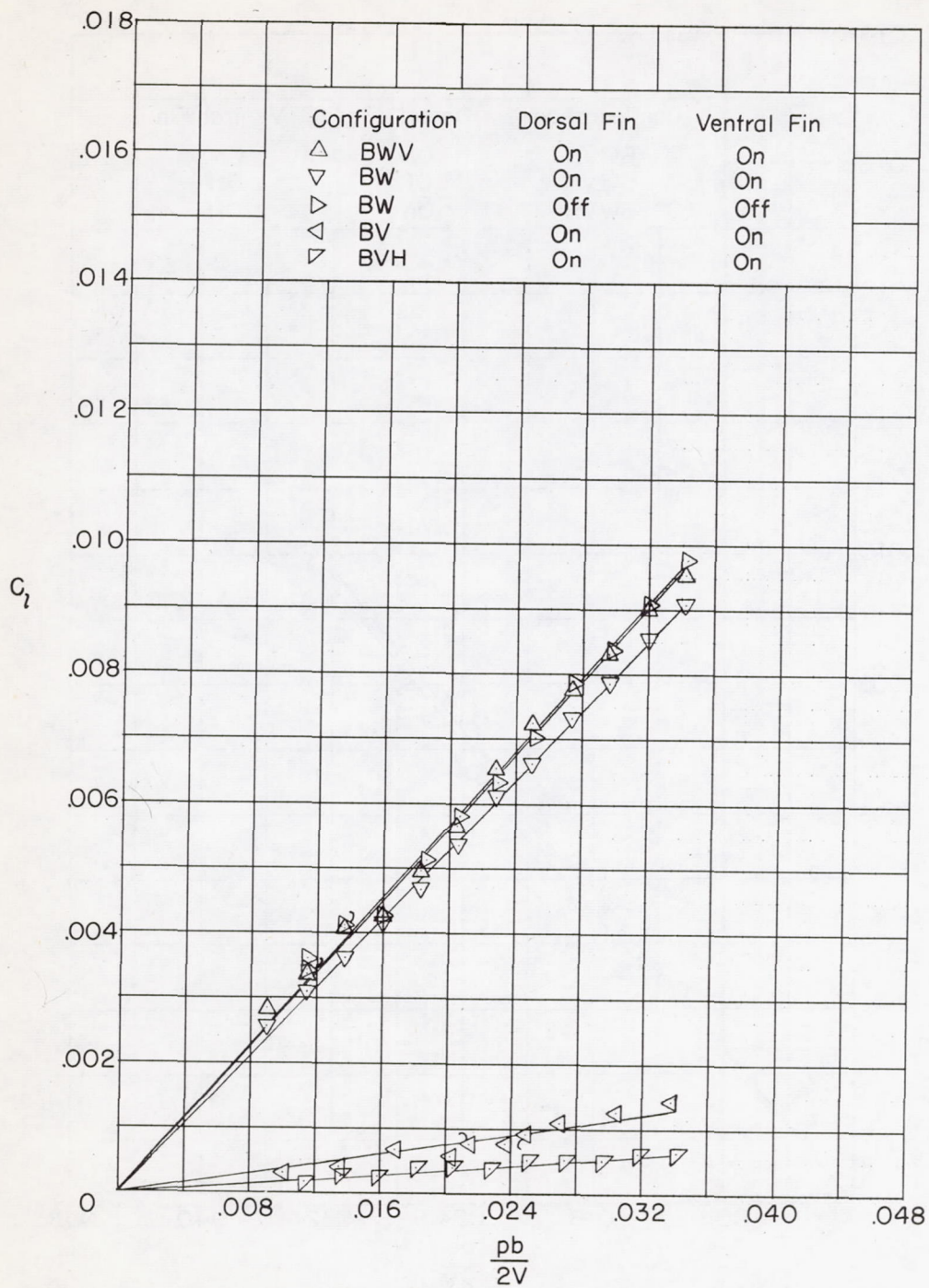
(a) Concluded.

Figure 3.- Continued.



(b)  $M = 1.94$ .

Figure 3.- Continued.



(b) Concluded.

Figure 3.- Continued.



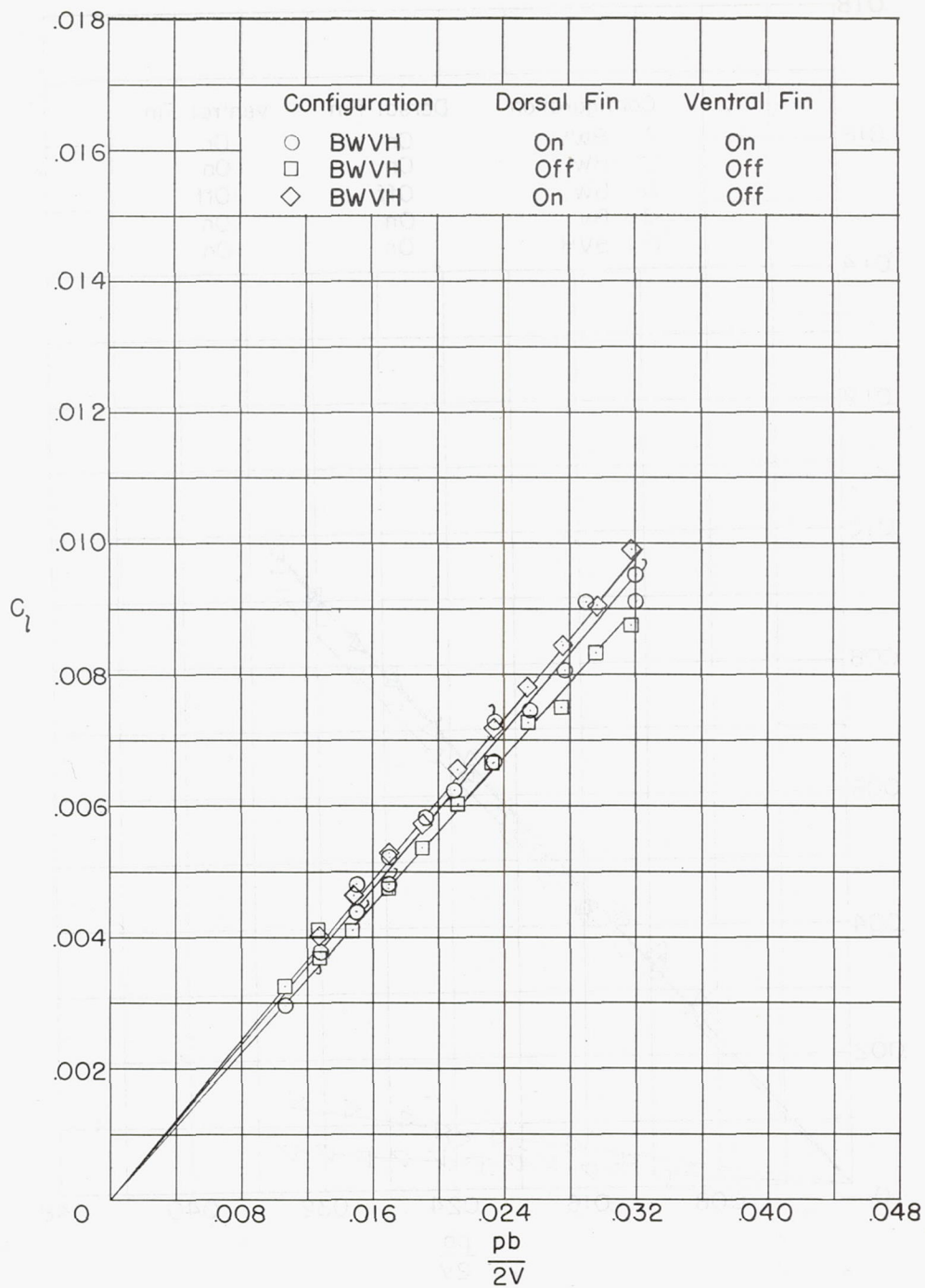
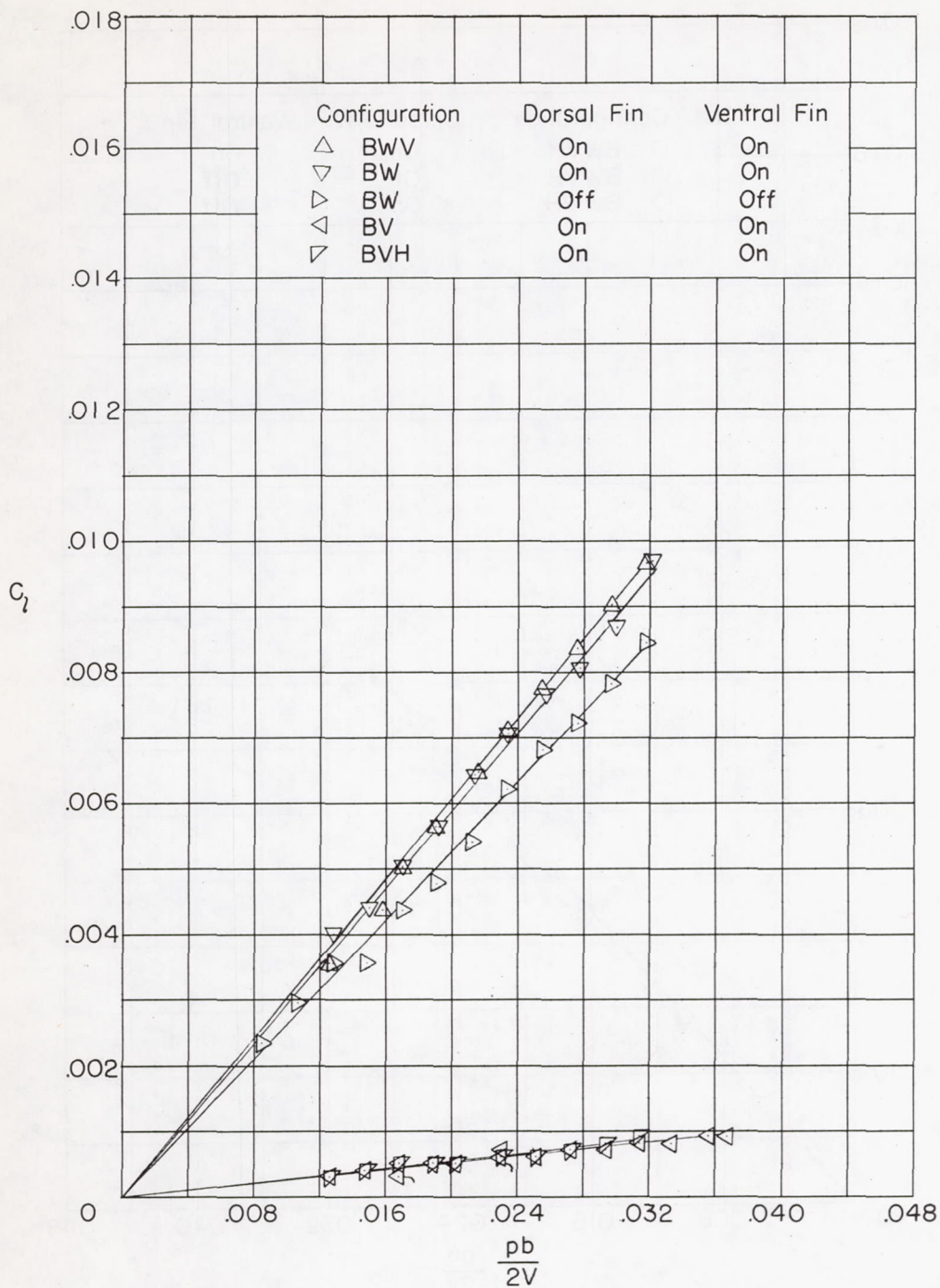
(c)  $M = 2.22$ .

Figure 3.- Continued.



(c) Concluded.

Figure 3.- Continued.

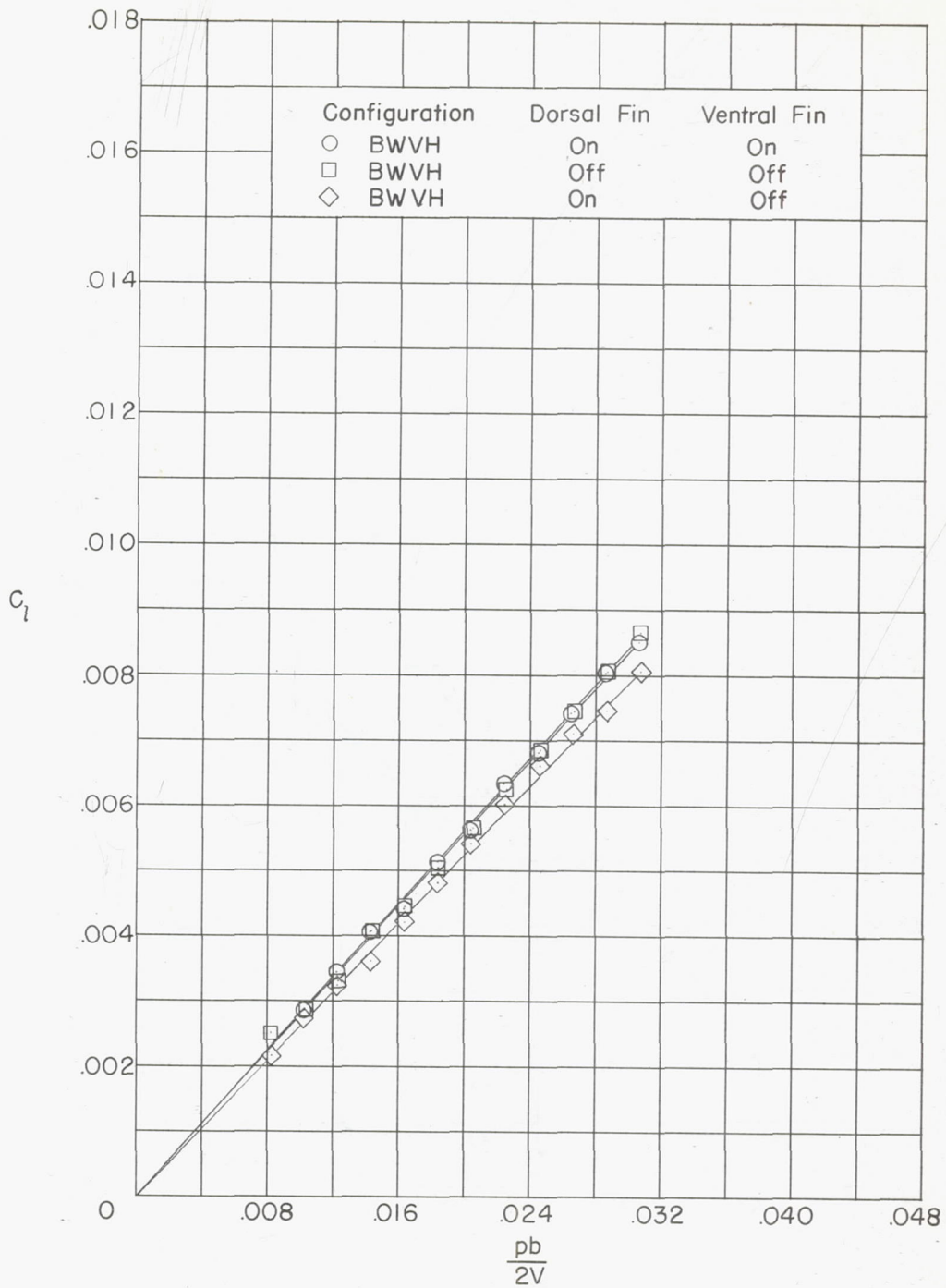
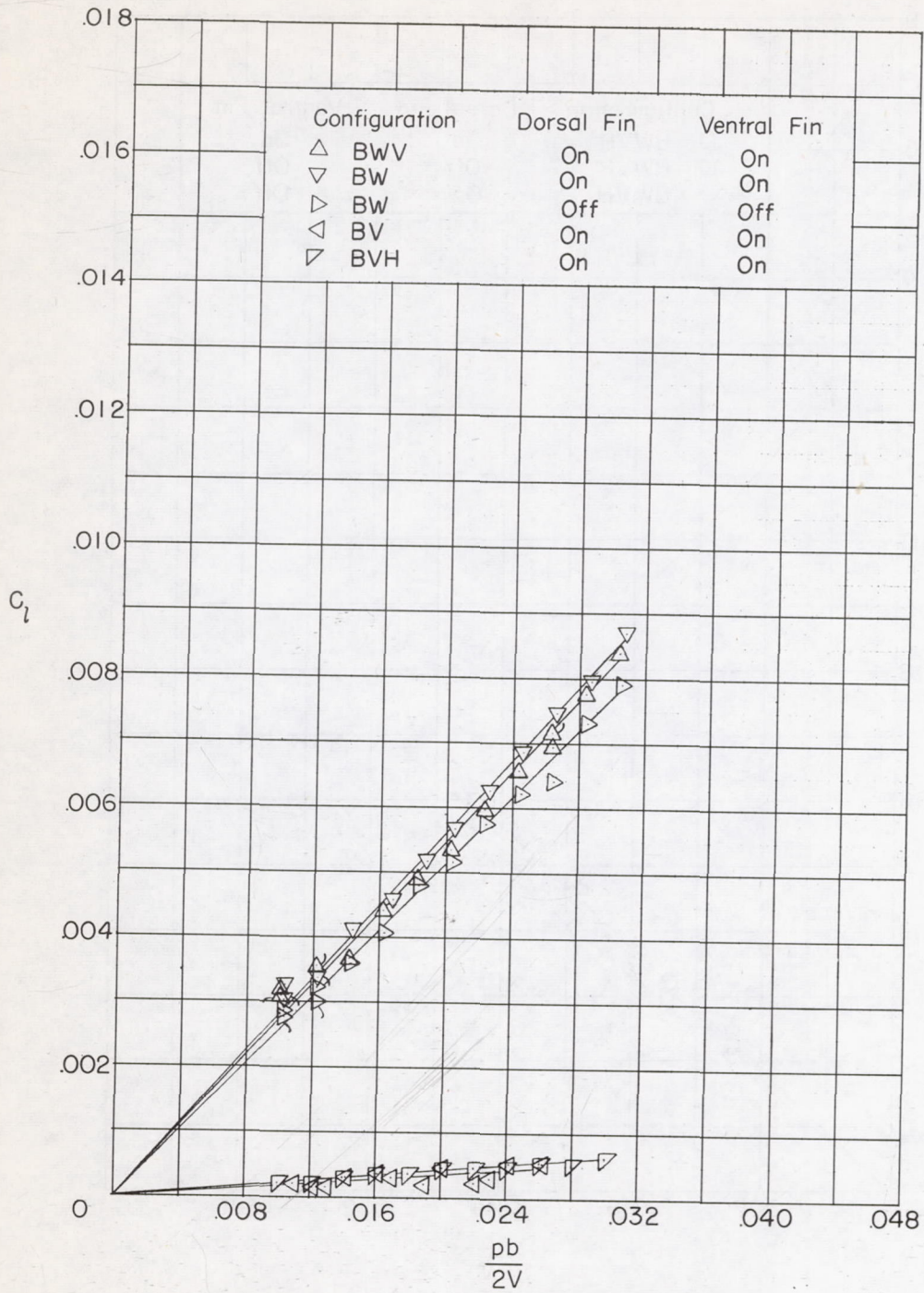
(d)  $M = 2.41$ .

Figure 3.- Continued.



(d) Concluded.

Figure 3.- Continued.

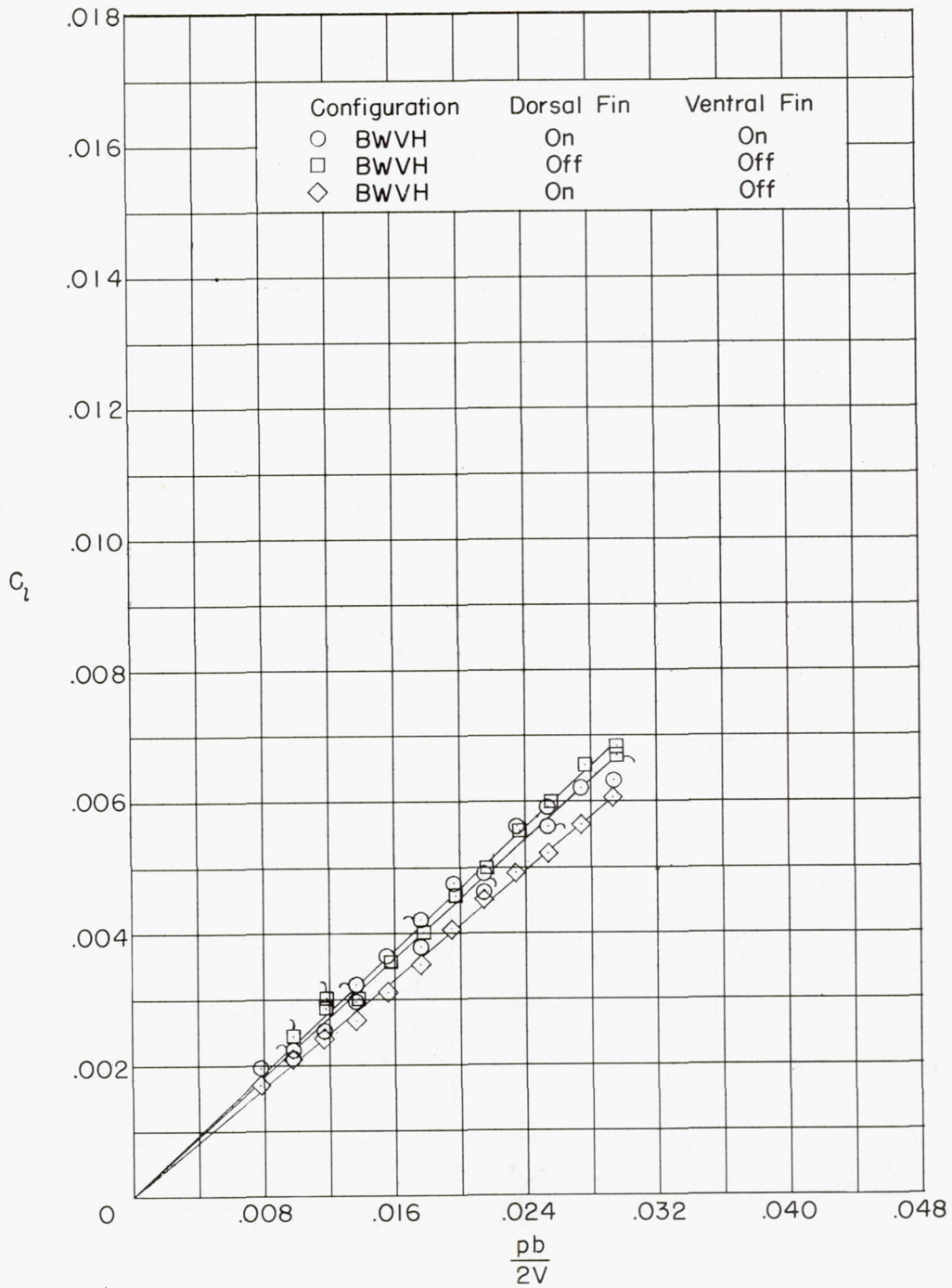
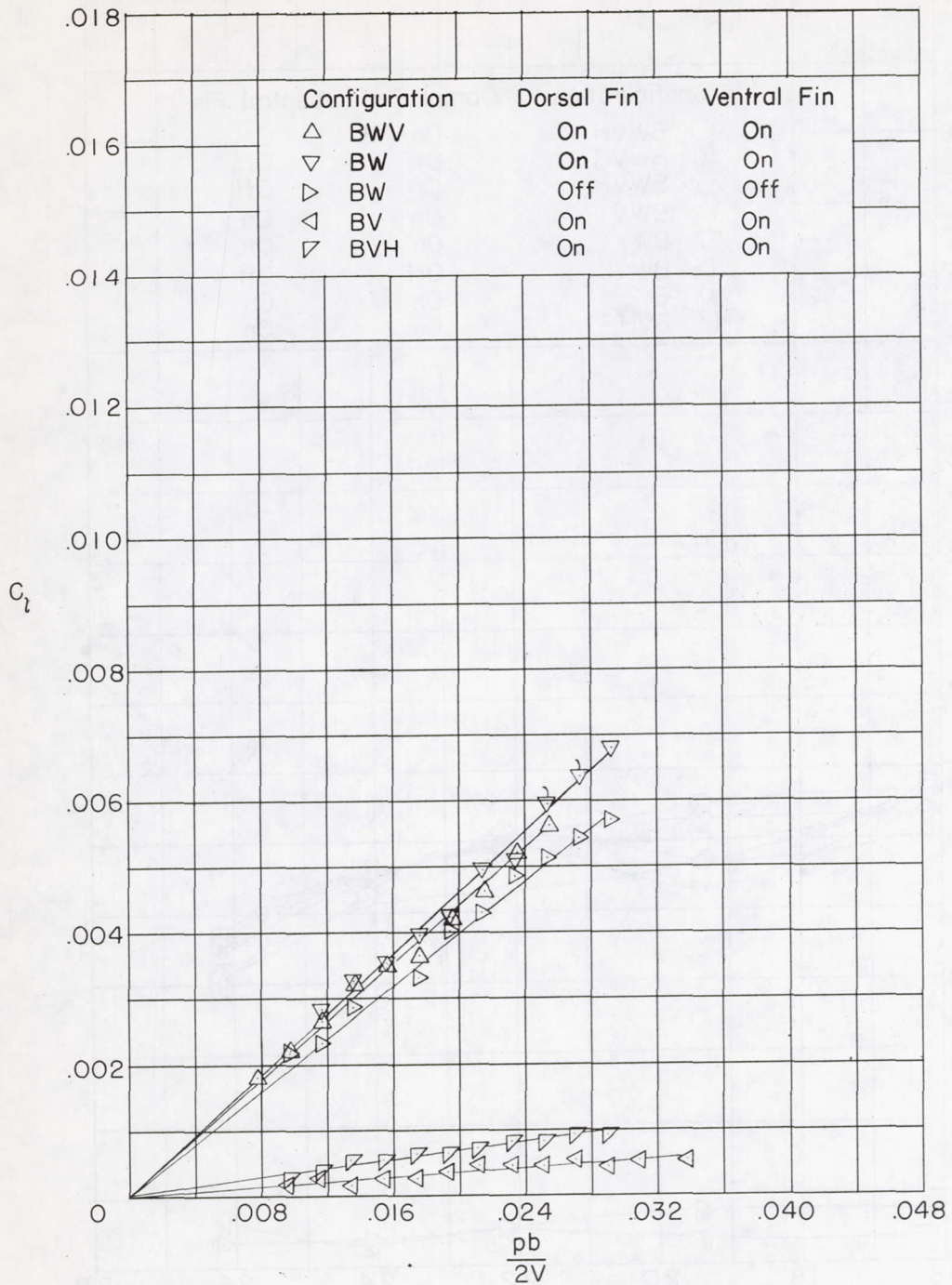
(e)  $M = 2.62$ .

Figure 3.- Continued.



(e) Concluded.

Figure 3.- Concluded.

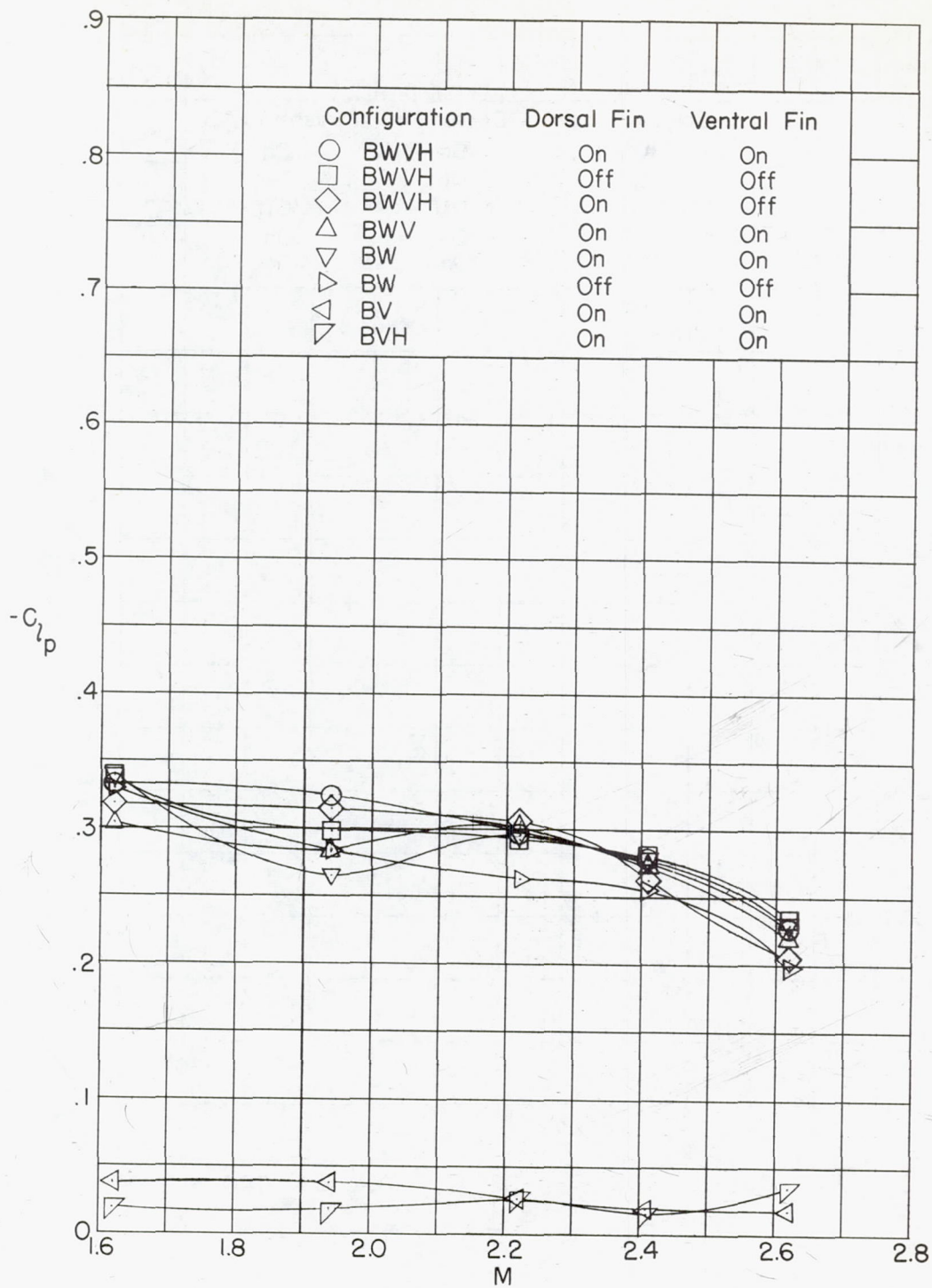
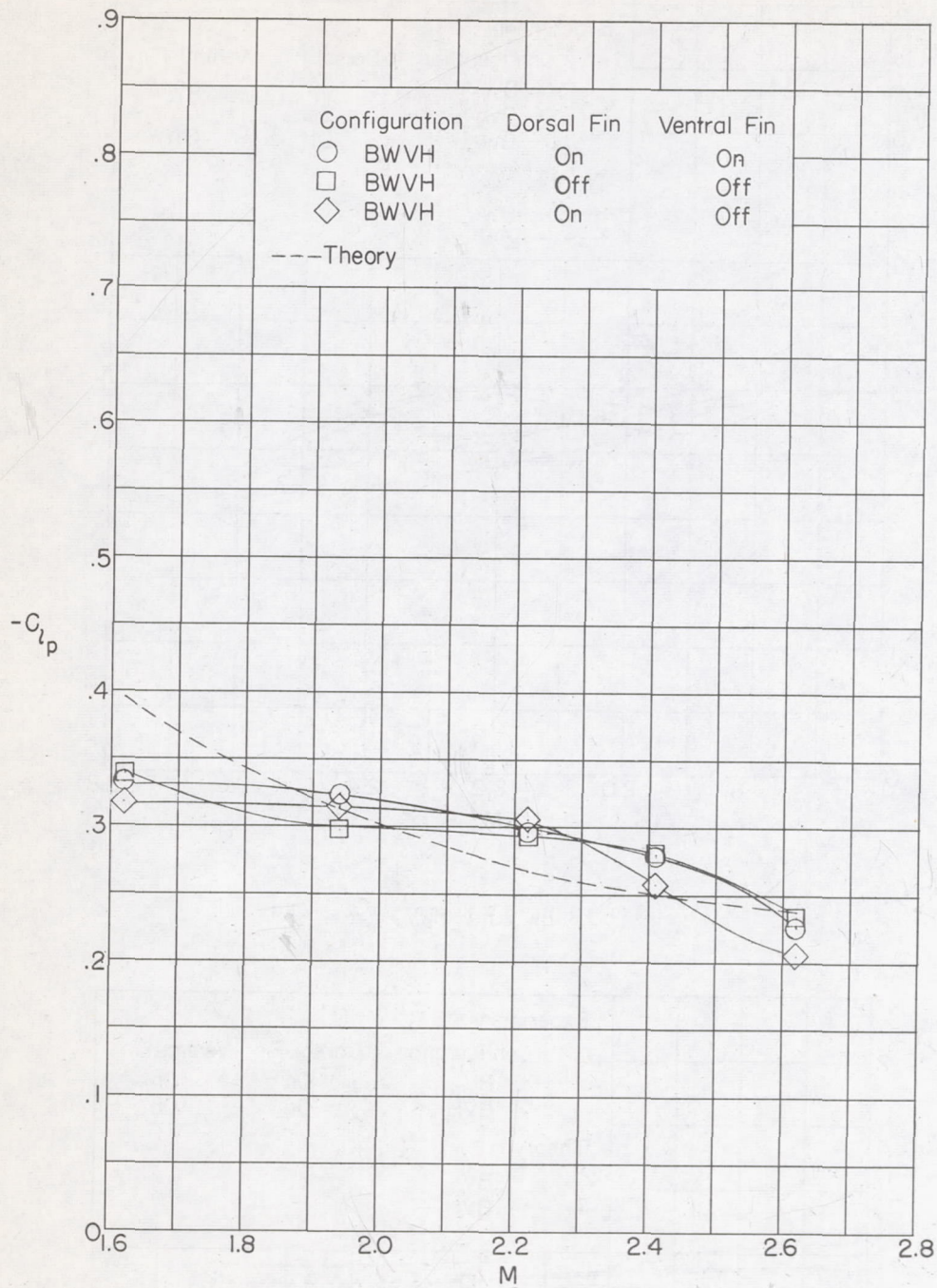


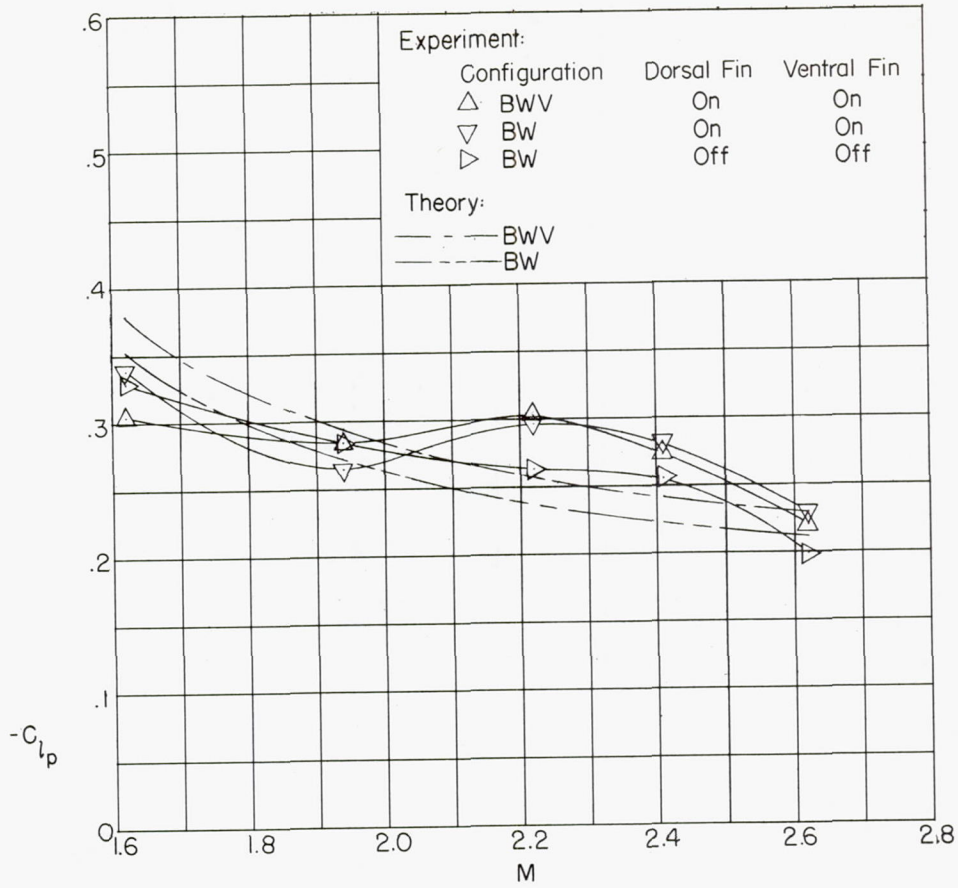
Figure 4.- Variation with Mach number of the damping in roll of the complete model and its components at zero angle of attack.



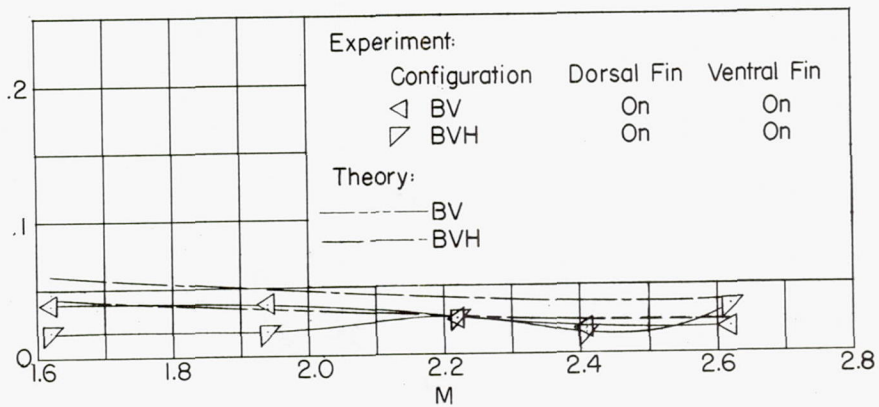
(a) BWVH.

Figure 5.- Variations with Mach number of the experimental and theoretical damping in roll at zero angle of attack.





(b) BW and BWV.



(c) BV and BVH.

Figure 5.- Concluded.